Journal of Robotics and Control (JRC)
Volume 6, Issue 1, 2025
ISSN: 2715-5072, DOI: 10.18196/jrc.v6i1.24472

Design and Implementation of a Backstepping Time Varying Sliding Mode Control for the Angular Velocity Control of a Hydraulic Rotary Actuator

Aws M. Abdullah [1*], Shibly A. Al-Samarraie [2], Hasan H. Ali [3], Arif A. Al-Qassar [4]
[1] University of Baghdad, Baghdad, Iraq
[2, 4] Control and Systems Engineering Department, University of Technology-Iraq, Baghdad, Iraq
[3] Directorate of Studies, Planning and Follow-up, Ministry of Higher Education and Scientific Research, Baghdad, Iraq
Email: [1] aws.abd@cois.uobaghdad.edu.iq, [2] shibly.a.alsamarraie@uotechnology.edu.iq, [3] hasan_h2002@yahoo.com, [4] arif.A.Alqassar@uotechnology.edu.iq
*Corresponding Author

Abstract—**The Backstepping Sliding Mode Control is a control technique used for controlling nonlinear systems. In this paper, the performance of the backstepping sliding mode controller schemes for the angular velocity control for a rotary actuator of an angular velocity control system that utilizes a novel hydraulic flow control method called inlet throttling was investigated. For the angular velocity dynamic, a linear state feedback with suitable high gain is designed as the virtual controller, where steady state error can be made arbitrarily small according to the gain value. A time varying sliding variable is then selected based on the designed virtual controller. The resulting control design is robust, and the maximum error of the angular velocity with respect to the desired value is derived via Lyapunov Function where its value can be controlled via suitable selections of the control parameters. The simulation results have been obtained based on the MATLAB software tools, which are system transient response, the performance and the robustness of the proposed control in forcing the angular velocity to track the reference value in spite of the uncertainty and disturbances in the system parameters were studied. The SMC is a more comprehensive solution for ensuring the best robustness of stability and performance for the model. The simulation results were generated using MATLAB software tools., which are system transient response, the proposed control performance and the robustness in forcing the angular velocity to track the reference value (100-2000 *RPM*) in spite of the uncertainty ($\underline{+}$10%) and disturbances (5-30 *N.m*) in the system parameters are studied.**

Keywords—Inlet Throttling Velocity Control System; Robust Control; Sliding Mode Control; Nonlinear Systems; Backstepping.

I. INTRODUCTION

The hydrostatic transmission systems are widely used in many applications because the system has high efficiency of the primary power source, the system is highly efficient even under partial load. The hydrostatic transmission systems have some problems in controlling the angular velocity for the rotary actuator, mainly because of the uncertainties in the parameters. This proposed hydrostatic transmission system consists mainly of the inlet-throttled pump, a throttling valve for adjusting the pump flow rate, and a rotary actuator, as shown in Fig. 2. The proposed system regulates the volume of fluid flow, which determines the velocity of the actuator [1][2]. A suitable robust controller is required in order to improve the performance and stability of the system. The sliding mode controller is a discontinuous robust controller and it is used with systems in presence of the disturbances and the variation in their parameters. Backstepping control design is used for designing the sliding mode controller. It depends on Lyapunov Functions, where they are used as guides to ensure stability at each stage, where help us understand the system's energy and guarantees that the control law drives the system towards a desired equilibrium point [3][4]. Table I gives a definition of system model.

TABLE I. A DEFINITION OF SYSTEM MODEL

Symbol	Quantity
x_1	Angular displacement
x_2	Angular velocity
x_3	Pressure supply
x_4	Valve openning area
x_5	Valve openning area ratio
x_6	Control action
P_A	Fluid pressures on the input of the actuator
P_B	Fluid pressures output of the actuator
P_A	Pressure supply
V_a	Volumetric displacement of the actuator per unit of rotation
η_{at}	Actuator Torque Efficiency
J	Mass moment of inertia
b	Viscous Damping Coefficient
θ	Angular displacement
$\dot{\theta}$	Angular velocity
$\ddot{\theta}$	Angular acceleration
V	Instantaneous volume of the chamber
V_0	Volume of the chamber when θ equals zero
β	Fluid bulk modulus of elasticity
Q_i	Volumetric flow rate from the charge pump
k_1	Coefficient of leakage
k_s	Valve Static Gain
t_d	Valve Time Delay
ω_n	Valve Natural Frequency
k_v	Constant of proportionality
A_v	Valve openning area
T_d	Disturbance Torque
ξ	Damping Ratio

II. LITERATURE REVIEW

Numerous studies investigated the use of the sliding mode controller to the hydraulic systems. A sliding mode adaptive controller SMAC strategy for VEHPS system. The proposed algorithm combines can effectively deal with unknown mismatched disturbances and parametric uncertainties in the systems was proposed in [4]. The results shown that the developed sliding mode adaptive controller scheme can achieve high-performance tracking under the condition of parametric uncertainties and unknown mismatched disturbances. A sliding mode based control concept for position regulation of hydraulic cylinder was proposed in [5]. It is mainly composed of three parts: A nonlinear state feedback controller linearizing the pressurization system, a cascaded control structure consisting of an inner force control and an outer position control loop and an observer. The proposed sliding mode controller based on RBF neural network. The sliding mode controller has high effectiveness. A robust controller for the electro-hydraulic position servo system with respect to system parameters uncertainty was presented in [6]. This controller has effectiveness and the robustness of the proposed control in forcing the position to track the reference value in spite of the uncertainty in system parameters. The uncertainty in hydraulic system was found to be mainly dependent of the variation on load mass (20 to 25 kg). A sliding mode observer approach to introduce the transformation scheme to make a system rational was implemented in [7]. The proposed fault estimation scheme essentially transforms the original system into two subsystems where the first one includes system uncertainties, but is free from sensor faults and the second one has sensor faults but without uncertainties. The effects of system uncertainties on the estimation errors of states and faults are minimized by integrating an $H\infty$ uncertainty attenuation level into the observer. A sliding mode control for two mass systems connected by a flexible joint. The proposed controller consists of separating the system into upper and lower subsystems, with estimating the perturbation for the upper subsystem via SMPE. The connection between the two subsystem controller was then made using the backstepping approach was proposed in [8]. The results exhibit that the proposed control method improves the performance of systems compared to conventional control methods. A Sliding Mode Control (SMC) for spool position control of a two stage electro–hydraulic servo valve was proposed in [9]. The simulation results show that spool position is controlled to a desired position without oscillation. An Adaptive Backstepping control design for controlling the angular position of Propeller-Driven Pendulum System (PDPS) in the presence of uncertainty in system parameters was proposed in [10]. The numerical results showed that the ABSC has better performance than STSMC and SMC in terms of steady-state errors and peak overshoot. A novel SMC method, which combined with PID control strategy (PIDSMC) to overcome the chattering problem of original SMC was developed in [11], where the original SMC discontinuous control input caused by the high-frequency switching gain is replaced with a continuous control input determined by a proportional-integral-derivative algorithm, which is consisted of the sliding surface and its derivative. A sliding mode controller with a neural network compensation scheme for electro-hydraulic systems subject to an unknown dead-zone input was developed in [12]. The boundedness and convergence properties of the closed-loop signals are proven using Lyapunov stability theory. Numerical results are presented in order to demonstrate the control system performance. A discontinuous projection-based ASMC controller with variable sliding surface gain for position tracking control of an electro-hydraulic servo system was presented in [13]. The dynamic model of the valve-controlled system is first established and the corresponding state-space equation is obtained. Next, the parametric adaptive estimation law and discontinuous projection algorithm were designed to estimate 289 unknown parameters of the EHSS, which could effectively overcome the influence caused by the parameter uncertainty. A sliding mode control for spool position control of a two stage electro–hydraulic servo valve was designed in [14]. The mathematical models of the system are described as 7 th and 3 rd order transfer functions with the derivatives of the control input. In order to incorporate the derivatives of the control input into the SMC design, the system was described with disturbance/uncertainty effects the proposed SMC design approach was simulated. The simulation results show that spool position is controlled to a desired position.

In the present work, the flow rate is controlled by the inlet throttling valve and a fixed displacement Pump. The stability and performance of the closed-loop situations were studied. The main purpose of this paper is to design a robust controller to the model system in spite of the variation in parameters values. A Backstepping sliding mode controller for closed-loop operation is utilized here to direct the actuator speed to the desired value with considering to parameters variation. The numerical simulations will demonstrate the effectiveness of the proposed controller with a broad range of the parameters variation. The multiplicative parametric uncertainty was studied, and the system's robustness was evaluated with six of the parameters are related to the valve dynamics which are the natural frequency, the damping ratio, the static gain, and the time delay, the other two parameters are the discharge coefficient and the fluid bulk modulus. All these parameter changes were considered within the range of (+/−) 10% of their nominal values. Time varying is used for chattering reducing and smoothing of time response. The present work organized as follows: firstly, it is introduced an overview to the sliding mode control. secondly the model of the hydraulic system is presented in next section. After that the required steps and assumptions for designing a sliding mode control is introduced, the numerical results of the effectiveness of the proposed controller and the conclusions are presented in the latter sections. The results offered good high robustness for global stability and performance for multi-step input and multiplicative uncertainty. The multiplicative uncertainty was analyzed depending on six uncertain parameters. These parameter changes were considered within the range of (+/−) 10% of their nominal values.

III. SLIDING MODE CONTROL AND BACKSTEPPING

Sliding modes as a phenomenon may appear in a dynamic system governed by ordinary differential equations with discontinuous right-hand sides. The term sliding mode first appeared in the context of relay systems.

In control systems, sliding mode control is a nonlinear control method that alters the dynamics of a nonlinear system by applying a discontinuous control signal or more rigorously, a set-valued control signal that forces the system to slide along a cross-section of the system's normal behavior [14]. The state-feedback control law is not a continuous function of time. Instead, it can switch from one continuous structure to another based on the current position in the state space. Hence, sliding mode control is a variable structure control method. The multiple control structures are designed so that trajectories always move toward an adjacent region with a different control structure, and so the ultimate trajectory will not exist entirely within one control structure. Instead, it will slide along the boundaries of the control structures [15][16]. The motion of the system as it slides along these boundaries is called a sliding mode and the geometrical locus consisting of the boundaries is called the sliding hyper surface. In the context of modern control theory, any variable structure system, like a system under SMC, may be viewed as a special case of a hybrid dynamical system as the system both flows through a continuous state space but also moves through different discrete control modes [17][18]. For example, $\ddot{x} = u$ can be explained in Fig. 1.

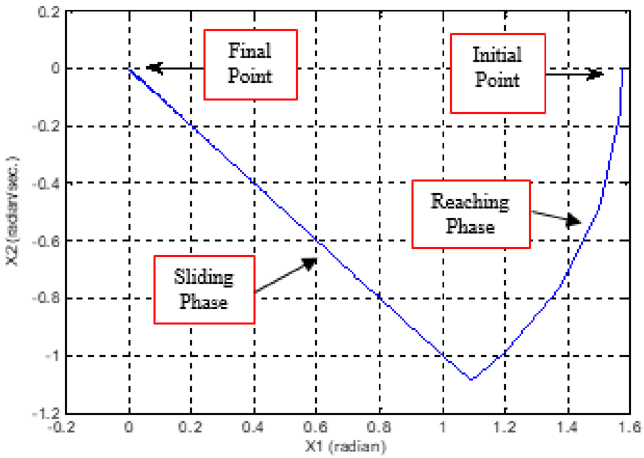

Fig. 1. The two stages of the state trajectory in SMC

The SMC is good at handling uncertainties and disturbances in the system because it focuses on keeping the state on the sliding surface, regardless of these external factors. The controller design process can be relatively straightforward compared to other techniques [19][20][21]. Backstepping works its way recursively from the inner states (closest to the control input) to the outer states (system output). At each level, it treats a specific state as a virtual control to design a control law for the lower-level subsystem. This virtual control helps achieve the desired behavior for the overall system [22][23]. Backstepping approach will enable us construction a sliding variable, which it is one of the two steps in designing a SMC. Backstepping ensures also the asymptotic stability or at least the ultimate bound on the steady state error for the objective variable. While deriving the control law (the second SMC design step) is made easily using Lyapunov Function which will ensure the attractiveness of the sliding manifold (the zero level of the sliding variable) [24][25][26].

IV. System Description

As shown in Fig. 2, the proposed hydrostatic transmission system utilizes inlet throttling valve for controlling the flow. Fixed displacement pump is utilized for pumping the flow during a desired pressure to rotary actuator. In Fig. 2, the hydrostatic transmission load that is moved by the actuator is shown as a rotary mass-spring-damper system with a load disturbance torque given by T_d. The mass moment of inertia, torsional spring rate, and the damping coefficient of the viscous for the load are shown in Fig. 1 by the symbols (J), (b), and (k) respectively.

The rotary actuator is shown with the fixed volumetric displacement per unit of rotation V_a and is connected to the rotating mass at the output shaft. In Fig. 1, the inlet-throttled pump is used to design an angular velocity control system because the flow in the proposed system is adjusted by a valve positioned at the pump inlet to reduce the energy losses across the valve, where shows fixed-displacement pump is sized according to its volumetric displacement V_P and is driven by an external power source (not shown in Fig. 2) at angular velocity ω_p. The pressure in the supply line of the charge pump is controlled using a high-pressure relief valve that is set at the desired supply pressure P_in. The charge pump itself is a fixed-displacement pump (usually a gear pump or a gerotor pump) that is used in conjunction with a relief valve for the purposes of providing makeup flow to the main fixed-displacement pump. The flow passages exist inherently within the system may also be designed for the purposes of directing fluid flow into the reservoir for cooling and filtration [27][28]. The Coolers and filters are not shown in Fig. 2.

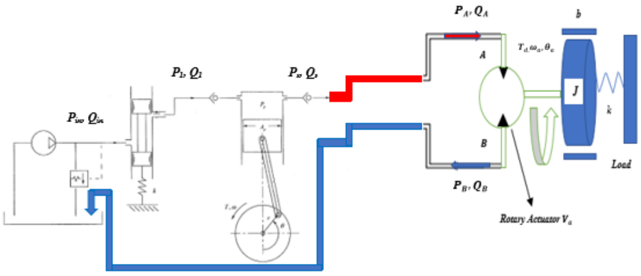

Fig. 2. Angular velocity control system for a rotary actuator

V. Dynamic Model of the System

The Dynamic Model of the System response will be created in order to realize the dynamic problems, so a mathematical model should be written for the system. The Basic components for model system are shown in Fig. 2. The mathematical equations of the plant system are derived. They include the torque dynamics as the rotary actuator's motion equation and pressure dynamics as the rate of pressure rise equation. The model has one inputs (A_v) and one disturbance (T_d)[29][30].

The torque dynamics can be expressed as follows [31][32][33]:

$$J\ddot{\theta} + b\dot{\theta} + k\theta = \eta_{at} V_a (P_A - P_B) - T_d \tag{1}$$

In Eq. (1), the torque exerted on the load by the rotary actuator is given by $\eta_{at} V_a (P_A - P_B)$ where η_{at} is the torque efficiency of the actuator. The load spring is typically excluded from velocity control analysis, i.e., $k = 0. \dot{\theta} = \omega$ and $P_s = P_A$ then eq. (1) becomes as Eq. (2) [34][35]:

$$J\ddot{\theta} + b\dot{\theta} = \eta_{at} P_s V_a - T_d \tag{2}$$

The rate of pressure rise equation can be expressed as follows:

$$\frac{V}{\beta}\dot{P}_s + k_1 P_s = \left(Q_i - V_a\dot{\theta}\right) \tag{3}$$

The instantaneous volume of the chamber can be expressed as follows [36][37]:

$$V = V_O + V_a\hat{\theta} \tag{4}$$

Also, $\hat{\theta}$ is considered here as the rotor rotation, therefore it can be expressed as follows:

$$\hat{\theta} = 2\pi(1 - \cos(\theta))/2 \tag{5}$$

where the inlet flow, Q_{in}, can be expressed as follows [38][39]:

$$Q_i = A_v C_d \sqrt{\frac{2P_i}{\rho}} \tag{6}$$

Therefore, equation (3), accordingly, becomes as follows,

$$\dot{P}_s = \frac{\beta}{V_O + V_a\hat{\theta}}\left(A_v C_d \sqrt{\frac{2P_i}{\rho}} - k_1 P_s - V_a\dot{\theta}\right) \tag{7}$$

The transfer function for the dynamics of the inlet throttled valve was experimentally determined and is shown in Eq. (8) [40][41]:

$$G_v(s) = \frac{A_v}{V_{in}} = \frac{k_v k_s e^{-s\tau_d}\omega_n^2}{s^2 + 2\xi\omega_n s + \omega_n^2} \tag{8}$$

The time delay introduces a serious limitation on the controller performance that can be achieved. The reason for that limitation is that the effect of the change of the input on the output will be delayed by an amount of time that is equal to the time delay. The time delay limits the closed-loop bandwidth frequency to be less than the reciprocal of the time delay as shown in Eq. (9) [42][43][44]:

$$\omega_b < \frac{1}{\tau_d} \tag{9}$$

Now, the mathematical model of the inlet-throttled angular velocity control for rotary actuator system, transformed into state space form as follows [45][46]:

$$\dot{\theta} = \omega \tag{10}$$

$$\dot{\omega} = -\frac{b}{J}\omega + \frac{\eta_{at}V_a}{J}P_s - \frac{T_d}{J} \tag{11}$$

$$\dot{P}_s = \frac{\beta}{V_O + V_a\hat{\theta}}\left(A_v C_d \sqrt{\frac{2P_i}{\rho}} - V_a\omega - k_1 P_s\right) \tag{12}$$

From Eq. (8), the second derivative of the valve opening area can be written as [47][48]:

$$\ddot{A}_v = -2\xi\omega_n\dot{A}_v - \omega_n^2 A_v + k_v k_s \omega_n^2 V_{in}(t - \tau_d) \tag{13}$$

The dynamic delay in $V_{in}(t - \tau_d)$ will be represented as a low pass filter,

$$\frac{V_{in}(t - \tau_d)}{V_{in}(s)} = e^{-s\tau_d} = \frac{1}{\tau_d s + 1} \tag{14}$$

or

$$\tau_d \dot{V}_{in}(t - \tau_d) + V_{in}(t - \tau_d) = V_{in}(t) \tag{15}$$

For the convenience of controller design, the following state variables are defined [49][50]:

$$\left[\theta \ \ \dot{\theta} \ \ P_s \ \ A_v \ \ \dot{A}_v \ \ V_{in}(t - \tau_d)\right]^T \rightarrow [x_1 \ \ x_2 \ \ x_3 \ \ x_4 \ \ x_5 \ \ x_6]^T$$

Valve input voltage V_{in} was considered here as the control input. So, set $V_{in} = u$, but $\boldsymbol{x_6}$ is considered as the new control signal, where this the actual control signal is the input voltage with delay time. The state space model with a control signal $\boldsymbol{x_6}$ will be more appropriate for designing a controller, as well as we can consider $\hat{\theta} = \hat{x}_1$, $d = -\frac{T_d}{J}$, thus then we can write complete the mathematical model as follows:

For the system model dynamic without inlet throttling valve dynamic,

$$\left.\begin{aligned} \dot{x}_1 &= x_2 \\ \dot{x}_2 &= -a_1 x_2 + a_2 x_3 + d \\ \dot{x}_3 &= -b_1 x_2 - b_2 x_3 + c x_4 \end{aligned}\right\} \tag{16}$$

And for the inlet throttling valve dynamic,

$$\left.\begin{aligned} \dot{x}_4 &= x_5 \\ \dot{x}_5 &= -\omega_n^2 x_4 - 2\xi\omega_n x_5 + k_v k_s \omega_n^2 x_6 \\ \dot{x}_6 &= -\frac{x_6}{\tau_d} + \frac{V_{in}(t)}{\tau_d} \end{aligned}\right\} \tag{17}$$

VI. Control Design and Stability Analysis

In this section, a convenience strategy to design a sliding mode controller will be presented. Firstly, we will divide the system in eq. (16) and eq. (17) into two subsystems; upper and lower subsystems. For each subsystem, the sliding variable is assigned based on the standard or 1st order SMC theory. The objective from the designed controller is to force state trajectories into the level zero for each sliding variable [51]. The loci of the points of the sliding variable level zero are called the sliding manifold or switching surface. After designing the SMC successfully, the state trajectory is directed towards the sliding manifold and then maintained it on this manifold for all future time. As a result, the state moves toward the origin or its neighborhood and stays there for all next time. This behavior is known as the reaching and sliding phases; which are depicted in Fig. 1 for a typical second-order system [52][53].

The uncertainty in the above equation (16) consists in the stiffness value; i.e., β and C_d can be written as:

Let $a_1 = \frac{b}{J}$, $a_2 = \frac{\eta_{at}V_a}{J}$, $b_1 = \frac{\beta V_a}{V_O + V_a\hat{x}_1}$, $b_2 = \frac{\beta k_1}{V_O + V_a\hat{x}_1}$, and $c = \frac{\beta C_d\sqrt{\frac{2P_i}{\rho}}}{V_O + V_a\hat{x}_1}$, then for $\beta = \beta_n + \Delta\beta$ and $C_d = C_{d_n} + \Delta C_d \Rightarrow b_1 = b_{1n} + \Delta b_1$, $b_2 = b_{2n} + \Delta b_2$, and $c = c_n + \Delta c$.

Accordingly, the above equation (16) can be expressed as follows:

$$\left.\begin{aligned} \dot{x}_1 &= x_2 \\ \dot{x}_2 &= -a_1 x_2 + a_2 x_3 + d \\ \dot{x}_3 &= -b_{1n} x_2 - b_{2n} x_3 + c_n x_4 + \delta_1 \end{aligned}\right\} \quad (18)$$

where $\delta_1 = -\Delta b_1 x_2 - \Delta b_2 x_3 + \Delta c x_4$.

Note that in Eq. (18) the subscription refers to the differential equations with nominal parameters, d and δ_1, are the disturbance and perturbation terms, which they act on the dynamics of the system model. The first and the second subsystems are referred to here as the upper and lower subsystems respectively [54][55].

The system was modeled with two degrees of freedom but actuated by only one control input (the valve input voltage), i.e. the control input does not exist in the upper subsystem dynamics (the system model without inlet throttled valve dynamic model). In this work, a nonlinear controller will be designed using the sliding mode control theory [56][57]. The sliding mode control will be designed for each degree of freedom separately with the considering of a perturbation term δ_1 , δ_2 and δ_3. Then using the Backstepping approach, the control law can be derived. The proposed controller will enforce a desired behavior on the overall system. Using the Back-stepping approach will enable one control action from controlling the system. As mentioned above, the SMC is designed for each subsystem; So, for the second line in Eq. (16) [58][59]

$$\dot{x}_2 = -a_1 x_2 + a_2 x_3 + d$$

Let x_3 be the virtual controller and denote it by v. Then let us propose the following virtual control law:

$$v = -H(t)e \quad (19)$$

where $e = x_2 - x_{2d}$ is the error function, and the $H(t)$ function i.e. defined as

$$H(t,\lambda) = \lambda * (1 - e^{-\alpha * t}) \quad (20)$$

where λ and α are positive constants which will be selected according to the required system response performance. Additionally, it can be noted that the virtual control is initially equal to zero and that due to the $H(t,\lambda)$ where $H(0,\lambda) = 0$ and moreover, $v \approx -\lambda * e$ after a sufficient period of time which depends on the value of α. For this reason, the virtual controller is taken as $-\lambda * e$ in the following analysis via Lyapunov Function [60][61]. So, let $V = \frac{1}{2}e^2$, then

$$\begin{aligned} \dot{V} &= e\dot{e} = e\dot{x}_2 = e\{-a_1 x_2 + a_2 v + d\} \\ &= e\{-a_1 x_2 - \lambda a_2 e + d\} = e\{-a_1 x_{2d} - (a_1 + \lambda a_2)e + d\} \end{aligned} \quad (21)$$

Since $(a_1 + \lambda a_2) > 0,\ \forall\lambda$, then according to for non-vanishing perturbation, we have

$$\begin{aligned} \dot{V} &\le -\min_{a_1,a_2}(a_1 + \lambda a_2)\, e^2 + |e|\left(\max_{a_1}|a_1 x_{2d}| + |d|\right) \\ &\le -(1-\beta)\min_{a_1,a_2}(a_1 + \lambda a_2)\, e^2, \quad \forall\ |e| \ge \frac{\left(\max_{a_1}|a_1 x_{2d}| + |d|\right)}{\beta * \min_{a_1,a_2}(a_1 + \lambda a_2)}, 0 < \beta < 1 \end{aligned} \quad (22)$$

Therefore, with the use of the virtual controller Eq. (19), the error between the angular velocity and the desired one (e) is ultimately bounded by

$$|e| \le b_e = \frac{|\delta|}{\beta * \min_{a_1,a_2}(a_1 + \lambda a_2)} \quad (23)$$

where b_e is the ultimate error bound and $|\delta| = \left(\max_{a_1}|a_1 x_{2d}| + |d|\right)$.

From Eq. (22), it can be shown that the required accuracy can be achieved via large enough value of the control parameter λ. Also, an important point can be noted here, is that the use of large value of λ will not lead to use a large control effort and that by using the time dependent function $H(t,\lambda)$ as mentioned above, the starting value of the virtual controller is equal to zero and the control parameter α will completely control the growth of the actual control value [62].

Since v is the virtual controller, so a sliding variable s_p is defined according to the Backstepping method by

$$s_p = x_3 - v \quad (24)$$

where s_p is initially equal to zero. The s_p is time varying since the time t is appeared explicitly in the virtual controller v. The time rate of change of s_p is given by

$$\dot{s}_p = -b_{1n} x_2 - b_{2n} x_3 + c_n x_4 + \delta_1 + \dot{H}(t)e + H(t)\dot{e} \quad (25)$$

where δ_1 is perturbation, let x_4 be the virtual controller and denoted it by u_p. Then to design the virtual control u_p , the following non-smooth Lyapunov Function was used:

$$V_p = \frac{1}{2}s_p^2 \quad (26)$$

To ensure the attractiveness of the sliding manifold ($s_p = 0$), the derivative of the Lyapunov function V_p must be negative definite as can be shown in the following steps;

$$\left.\begin{aligned} \dot{V}_p &= s_p * \dot{s}_p \\ &= s_p * [-b_{1n} x_2 - b_{2n} x_3 + c_n u_p + \delta_1 + \dot{H}(t)e + H(t)\dot{e}] \end{aligned}\right\} \quad (27)$$

Let

$$u_p = (u_{pn} + u_{ps})/c_n \quad (28)$$

where the first term in the control law is u_{pn} which it is taken here as,

$$u_{pn} = b_{1n} x_2 + b_{2n} x_3 - \dot{H}(t)e \quad (29)$$

while u_{ps} is taken here as,

$$u_{ps} = -k_p * s_p \quad (30)$$

After substituting the proposed controller in $\dot{V}_p$, we obtained;

$$\left.\begin{aligned} \dot{V}_p &= s_p * \dot{s}_p \\ &= s_p * [-b_{1n} x_2 - b_{2n} x_3 + u_{pn} + u_{ps} + \delta_1 + \dot{H}(t)e + H(t)\dot{e}] \\ \dot{V}_p &= s_p * [-k_p s_p + \delta_1 + H(t)\dot{e}] \\ \dot{V}_p &\le -k_p|s_p|^2 + |s_p||\,\delta_1 + H(t)\dot{e}| \\ \dot{V}_p &\le -k_p(1-\beta_1)\, s_p^2 \qquad \forall\ |s_p| > \frac{|\,\delta_1 + H(t)\dot{e}|}{k_p \beta_1} \end{aligned}\right\} \quad (31)$$

where, $0 < \beta_1 < 1$. Therefor, s_p is ultimately bounded by $b_p = \frac{|\,\delta_1 + H(t)\dot{e}|}{\beta_1 k_p}$.

Note that, since s_p is initially equal to zero, then it will growth to the ultimate bound b_p, which it is inversely proportional to the gain k_p. Accordingly, s_p can be made small enough using large value of k_p.

As we mentioned above, u_p is considered as the virtual control for the system dynamic which is given by Eq. (16). To derive the actual control system signal, the throttling valve dynamic is included Eq. (17), and we need again to rewrite it considering the nominal and the perturbation terms [63][64].

The uncertainty in Eq. (17) consists in the stiffness value too; i.e., ξ, ω_n, k_s and τ_d can be written as:

$\xi = \xi_n + \Delta\xi$, $\omega_n = \omega_{n_n} + \Delta\omega_n$, $k_s = k_{s_n} + \Delta k_s$ and $\tau_d = \tau_{d_n} + \Delta\tau_d$

So, Eq. (16-b) can be expressed as follows:

$$\left.\begin{array}{c} \dot{x}_4 = x_5 \\ \dot{x}_5 = -2\xi_n\omega_{n_n}x_5 - \omega_{n_n}^2 x_4 + k_{v_n}k_{s_n}\omega_{n_n}^2 x_6 + \delta_2 \\ \dot{x}_6 = -\dfrac{x_6}{\tau_{d_n}} + \dfrac{V_{in}(t)}{\tau_{d_n}} + \delta_3 \end{array}\right\} \quad (32)$$

where $\delta_2 = -2\Delta(\xi\omega_n)x_2 - \Delta\omega_n^2 x_4 + k_v\Delta(k_s\omega_n^2)x_6$ and $\delta_3 = -\Delta\left(\frac{1}{\tau_d}\right)x_6 + \Delta\left(\frac{1}{\tau_d}\right)V_{in}(t)$.

Note that in Eq. (32), the subscription refers to the functions with nominal parameters, δ_2, δ_3 are the perturbation terms, which they act on the second is the valve dynamic model respectively. the second subsystems are referred to them here as the lower subsystems respectively [65][66]. The control input does exist in the lower subsystem dynamics, in the inlet throttled valve dynamic model, which is affected by the perturbation δ_2, δ_3.

In a similar way, the following steps are adapted for the lower subsystem which it given in Eq. (32). Let e_v be defined as:

$$e_v = x_4 - u_p \quad (33)$$

And it's the time rate of change is given by

$$\dot{e}_v = \dot{x}_4 - \dot{u}_p \quad (34)$$

As can be seen that the relative degree between e_v and the valve input voltage V_{in} is two, where V_{in} does not appear in x_5 control. Accordingly, we must define the following sliding variable as an output with relative degree one can be defined as [67][68]:

$$s = \dot{e}_v + \lambda_v e_v \quad (35)$$

And the time rate of change of s is

$$\dot{s} = -2\xi_n\omega_{n_n}x_5 - \omega_{n_n}^2 x_4 + k_{v_n}k_{s_n}\omega_{n_n}^2 x_6 + \delta_2 - \ddot{u}_p + \lambda_v\dot{e}_v \quad (36)$$

where δ_2 is perturbation and $\lambda_v > 0$ is a design parameter [69][70]. To evaluate $\dot{e}_v$ we need to determine the time rate of change of u_p, and since $\dot{u}_p$ is uncertain, therefore we need to estimate it through the sliding mode observer in Appendix (A) [71]-[74].

Again, consider x_6 be the virtual controller and denote it by u_v. Then to design the control u_v , we use the following non-smooth Lyapunov Function [75][76]:

$$V = \frac{1}{2}s^2 \quad (37)$$

To ensure the attractiveness of the sliding manifold ($s = 0$), k_v is selected such that the derivative of the lyapunov function V_v is negative definite as can be shown in the following steps [77][78];

$$\left.\begin{array}{c} \dot{V}_v = sgn(s) * \dot{s} \\ = sgn(s) * \left[-\omega_{n_n}^2 x_4 - 2\xi_n\omega_{n_n}x_5 + k_{v_n}k_{s_n}\omega_{n_n}^2 u_v + \delta_2 - \ddot{u}_p + \lambda_v\dot{e}_v\right] \\ = s * \left[-\omega_{n_n}^2 x_4 - 2\xi_n\omega_{n_n}x_5 + k_{v_n}k_{s_n}\omega_{n_n}^2 u_v + \hat{\delta}_2\right] \end{array}\right\} \quad (38)$$

where $\hat{\delta}_2 = \delta_2 - \ddot{u}_p + \lambda_v\dot{e}_v$.

Now, let

$$u_v = (u_{vn} + u_{vs})/(k_{v_n}k_{s_n}\omega_{n_n}^2) \quad (39)$$

Let the first term in the control law is u_{vn} is taken here as:

$$u_{vn} = \omega_{n_n}^2 x_4 + 2\xi_n\omega_{n_n}x_5 \quad (40)$$

While the second term in the control law is u_{vs} is taken as

$$u_{vs} = -k_v * H_1(t) * s \quad (41)$$

Here the $H_1(t)$ function is a positive function defined as

$$H_1(t) = (1 - e^{-\alpha_1 * t}) \quad (42)$$

where α_1 is positive constant which will be selected according to the required system response performance. Accordingly, $\dot{V}_v$ becomes [79][80];

$$\left.\begin{array}{c} \dot{V}_v = s * \left[-k_v * H_1(t) * s + \hat{\delta}_2\right] \\ \leq -k_v * H_1(t) * s^2 + |s||\hat{\delta}_2| \\ \leq -(1-\beta_2)k_v * H_1(t) * s^2, \ \forall |s| > \dfrac{|\hat{\delta}_2|}{k_v H_1(t)\beta_2} \quad 0 < \beta_2 < 0 \end{array}\right\} \quad (43)$$

Again, as in the previous design steps, s is ultimately bounded by $b_v = \frac{|\hat{\delta}_2|}{\beta_2 k_v H_1(t)}$.

Not that, the actual control input voltage $V_{in}(t)$ can be taken equal to the designed controller u_v and study the effect of the delay in the valve system dynamic through the simulations and in this case the virtual controller x_6 will take a period of time to follow the designed controller u_v . one can reduce the delay time effect via modifying the relation between $V_{in}(t)$ and u_v in the following form [81][82][83]:

$$V_{in}(t) = x_6\left\{1 - \frac{\tau_{d_n}}{\hat{\tau}_{d_n}}\right\} + \frac{\tau_{d_n}}{\hat{\tau}_{d_n}}u_v \quad (44)$$

where $\hat{\tau}_{d_n}$ is a design parameter.

Now we need to explore how the ultimate bounds b_v and b_p affected the main design objective which it is the ultimate bound b_e on the error function e. The following proposition give the answer about this question [84][85].

Proposition 1: Consider the control law for the Rotary Actuator system and the ultimate bounds b_e, b_p and b_v as given by Eq. (23), Eq. (31) and Eq. (43) respectively. The actual ultimate bound b_e on the error function e after considering the complete control design, with $\beta = \beta_1 = \beta_2 = 1$, is given by

$$\tilde{b}_e = \frac{\max\limits_{a_1,a_2}\left\{(|a_1 x_{2d}| + |d|) + a_2\left(\frac{\frac{|\hat{\delta}_2|}{\lambda_v k_v} + |\delta_1 + \dot{e}|}{k_p}\right)\right\}}{\min\limits_{a_1,a_2}(a_1 + \lambda a_2)} \quad (45)$$

Proof: first we derive the ultimate bound b_e by considering the ultimate bound on the sliding variable s_p. So, instead of taking the ideal case where $s_p = 0$ which leads to consider x_3 equal to the virtual control v, x_3 is taken as $x_3 = v + s_p$, and substitute in the Lyapunov function in Eq. (21). s_p is added with perturbation term δ, and consequently from Eq. (23), the ultimate bound b_e [86][87]

$$\hat{b}_e = \frac{\max\limits_{a_1,a_2}\{(|a_1 x_{2d}| + |d|) + a_2 b_p\}}{\min\limits_{a_1,a_2}(a_1 + \lambda a_2)} \quad (46)$$

Again, by considering that the sliding variable $s = \dot{e}_v + \lambda_v e_v$ will be not equal to zero, but instead it is bounded by b_v, and accordingly, e_v becomes bounded by [88];

$$|\lambda_v e_v| \le |s| \le b_v \quad \Rightarrow \quad |e_v| \le \frac{|\hat{\delta}_2|}{\beta_3 \lambda_v k_v}$$

Now we can evaluate b_p by considering that $x_4 = u_p + e_v$ in the Lyapunov analysis in Eq. (26) to Eq. (31), $|\hat{\delta}_1|$ is equal to $b_p = \frac{|\hat{\delta}_1|}{\beta_1 k_p}$, where $|\hat{\delta}_1| = |c_n|e_v| + \delta_1 + H(t)\dot{e}|$ and therefore b_p becomes

$$b_p = \frac{c_n|e_v| + |\delta_1 + H(t)\dot{e}|}{\beta_1 k_p} = \frac{c_n\frac{|\hat{\delta}_2|}{\beta_3\lambda_v k_v} + |\delta_1 + H(t)\dot{e}|}{\beta_1 k_p} \quad (47)$$

Eventually, b_e becomes

$$\tilde{b}_e = \frac{\max\limits_{a_1,a_2}\left\{(|a_1 x_{2d}| + |d|) + a_2\left(\frac{c_n\frac{|\hat{\delta}_2|}{\beta_3\lambda_v k_v} + |\delta_1 + H(t)\dot{e}|}{\beta_1 k_p}\right)\right\}}{\min\limits_{a_1,a_2}(a_1 + \lambda a_2)} \quad (48)$$

And with $\beta = \beta_1 = \beta_2 = 1$, the $\tilde{b}_e$ is as given in Eq. (45).

The above result revels that with large enough control gains λ, k_p and λ_v, the ultimate bound on the error function $\tilde{b}_e$ can made arbitrarily small [89].

VII. Results and Discussion

The dominant parameters in the system model of the proposed hydrostatic transmission (HST) systems are given in Table II, which presents the values of the system model parameters.

The parameters in the robust controller are given in Table III, which presents the values of the controller parameters.

TABLE II. Model Parameters

Dimensional Quantity	Definition	The value (SI units)
k_s	static gain of the valve	0.72
k_1	Leakage Coefficient	$0.14*10^{-11}\ m^4.s/kg$
k_v	constant of proportionality	$3.75*10^{-6}\ m^2/volt$
P_s	Pressure Supply	$25*10^6\ N/m^2$
cd	Discharge Coefficient	0.62
P_i	input pressure	$2*10^6\ N/m^2$
V_o	Actuator Volume	$8.2*10^{-6}\ m^3$
J	Mass moment of inertia	$0.013\ kg.m^2$
ρ	fluid density	$850\ kg/m^3$
b	viscous damping coefficient	$0.025065\ kg.m^2/s$
V_a	Volumetric displacement of the actuator	$1.3051*10^6\ m^3/rad$
β	Fluid Bulk Modulus	$1*10^9\ N/m^2$
η_{at}	Actuator mechanical Efficiency	0.95
ω_n	Valve Natural Frequency	$85\ rad/s$
τ_d	time delay of valve	0.015 s
ξ	Damping Ratio of the Valve	0.8

TABLE III. The Definitions of Quantities of Controller

Parameters	Value	Model Type
λ	1.5×10^4	Control Low of Upper Subsystem
α	25×10^{-4}	
k_p	17.5×10^3	
λ_v	0.5	Control Low of Lower Subsystem
α_1	1	
k_v	5×10^{-3}	
ku	100	Estimator
α_2	0.5	

The parameters of the switching function in Eq. (22) and switching function in Eq. (35) are chosen depending on Table III. The reduced dynamics, when the states reach zero value in a finite time, is exponentially asymptotically stable. In deriving the sliding mode control laws in Eq. (28) and Eq. (39), the nominal system parameters are considered as well as the disturbances and uncertainties. The sliding mode controller will definitely overcome system uncertainties for suitable control laws. This design chose the desired velocity as $1600\ RPM$ at zero second with disturbance torque $25\ N.m$, was applied to the actuator, as an external load at 35 seconds, where the effects of the disturbance torque on the angular velocity ω_a, desired pressure P_s, valve opening area A_V, input voltage V_{in}, are shown in the Fig. 3 to Fig. 16 for three cases as followed:

Case1: Constant desired angular velocity. The desired angular velocity of actuator to $\mathrm{x_{2d}} = 1600\ \mathrm{RPM} \rightarrow 167.5516\ \mathrm{rad/s}$ is supplied as a set point. As a result, the angular velocity reaches the final value at steady state for the robust controller (CSMC) with the supplied disturbance torque effects ($25\ N.m$) is applied in the time = 35 sec at steady state with high stability and performance as shown in Fig. 3. The response results of the robust controller are shown in Table IV.

TABLE IV. Results of Velocity Time Response with Robust Controller

Robust Controller	Steady state value	Error steady State	Rise Time	Max. Overshoot (%)	Steady state value (with disturbance)
CSMC	167.3 rad/sec	0.2516 rad/sec	1.885 sec	0	166.8 rad/sec

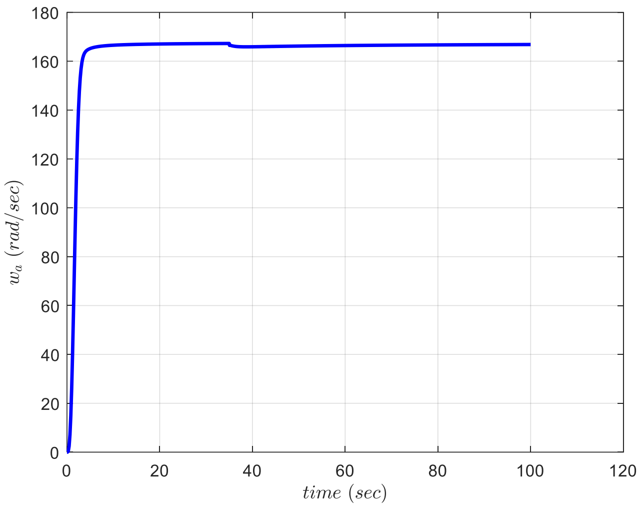

Fig. 3. The velocity time response of closed-loop with robust controller with torque disturbances effects

The desired angular velocity of actuator to $x_{2d} = 1600$ RPM $\rightarrow 167.5516$ rad/s is supplied as a set point. As a result, the pressure supply reaches the final value at steady state for the robust controller (CSMC) with the supplied disturbance torque $(25\ N.m)$ effects is applied in the time = 35 sec at steady state with high stability and performance as shown in Fig. 4. The response results of the robust controller are shown in Table V.

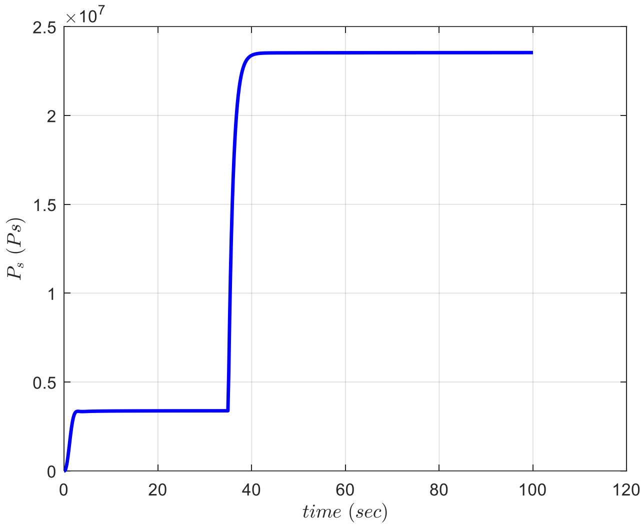

Fig. 4. The pressure supply time response of closed-loop with robust controller with torque disturbances effects

TABLE V. RESULTS OF PRESSURE SUPPLY TIME RESPONSE WITH ROBUST CONTROLLER

Robust Controller	Steady state value	Rise Time	Max. Overshoot (%)	Steady state value (with disturbance)
CSMC	3.381 MP	1.465 sec	0	23.54 MP

The desired angular velocity of actuator to $x_{2d} = 1600$ RPM $\rightarrow 167.5516$ rad/s is supplied as a set point. As a result, the valve opening area reaches the final value at steady state for the robust controller (CSMC) with the supplied disturbance torque $(25\ N.m)$ effects is applied in the time = 35 sec at steady state with high stability and performance as shown in Fig. 5. The response results of the robust controller are shown in Table VI.

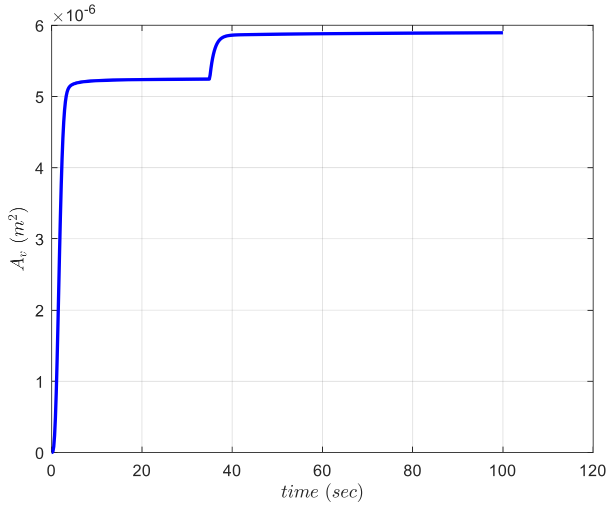

Fig. 5. The valve opening area time response of closed-loop with robust controller with torque disturbances effects

TABLE VI. RESULTS OF VALVE OPENING AREA TIME RESPONSE WITH ROBUST CONTROLLER

Robust Controller	Steady state value	Rise Time	Max. Overshoot (%)	Steady state value (with disturbance)
CSMC	$5.24 \times 10^{-6}\ m^2$	1.9 sec	0	$5.89 \times 10^{-6}\ m^2$

The desired angular velocity of actuator to $x_{2d} = 1600$ RPM $\rightarrow 167.5516$ rad/s is supplied as a set point. As a result, the control action (V_{in} with delay time) reaches the final value at steady state for the robust controller (CSMC) with the supplied disturbance torque $(25\ N.m)$ effects is applied in the time = 35 sec at steady state with high stability and performance as shown in Fig. 6. The response results of the robust controller are shown in Table VII.

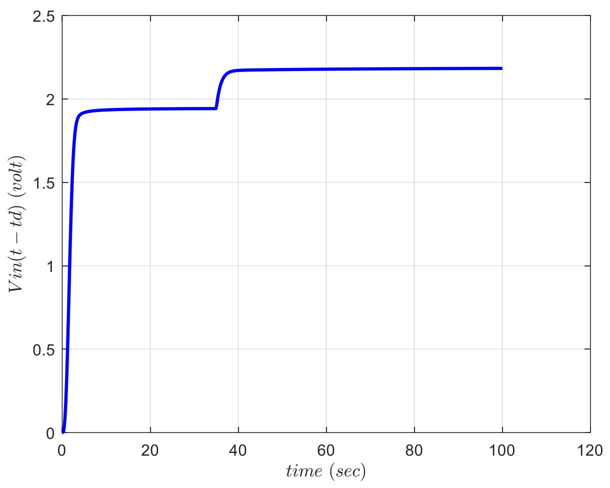

Fig. 6. The control action time response of closed-loop with robust controller with torque disturbances effects

TABLE VII. RESULTS OF VALVE OPENING AREA TIME RESPONSE WITH ROBUST CONTROLLER

Robust Controller	Steady state value	Rise Time	Max. Overshoot (%)	Steady state value (with disturbance)
CSMC	1.942 volt	1.914 sec	0	2.183 volt

The desired angular velocity of actuator to $x_{2d} = 1600\ \text{RPM} \rightarrow 167.5516\ \text{rad/s}$ is supplied as a set point. As a result, the valve input voltage (V_{in}) reaches the final value at steady state for the robust controller (CSMC) with the supplied disturbance torque ($25\ N.m$) effects is applied in the time $= 35$ sec at steady state with high stability and performance as shown in Fig. 7. The response results of the robust controller are shown in Table VIII.

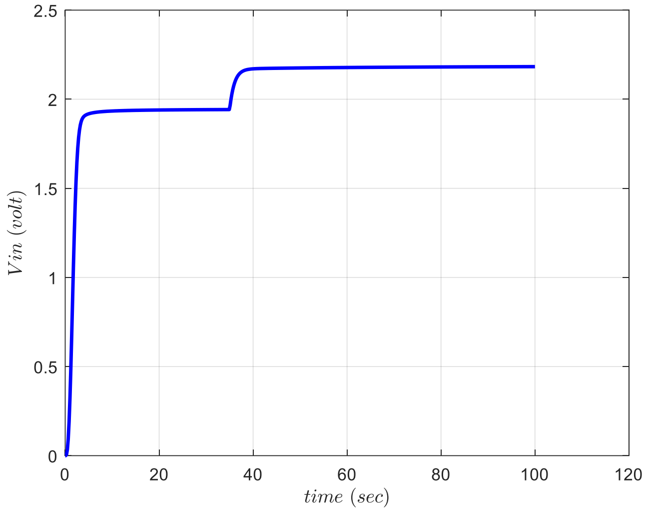

Fig. 7. The valve input voltage time response of closed-loop with robust controller with torque disturbances effects

TABLE VIII. RESULTS OF VALVE INPUT VOLTAGE TIME RESPONSE WITH ROBUST CONTROLLER

Robust Controller	Steady state value	Rise Time	Max. Overshoot (%)	Steady state value (with disturbance)
CSMC	1.942 volt	1.8885 sec	0	2.183 volt

The proposed sliding mode controller will guide the states to the sliding surface in considerably proper time. This is known as the reaching time which it relates to the control parameters of the switching functions form where the time required to regulate the switching function first and second respectively. After reaching sliding manifold $s_p = 0$ the error states is regulated asymptotically to the origin. The sliding variables s_p are plotted in Fig. 8 with high stability and performance with reaching time $(t_r) = 7\ sec$. The plot is smooth where the chattering effect is eliminated from the sliding mode control. The effects of the disturbance is represented on s_p in the Fig. 8 in the time of 35 second.

Case2: Piecewise constant desired angular velocity. At the time = 100 s, at steady state, this design chose increasing the set point with $x_{2d} = 36.6519\ \text{rad/s}$. As a result, the angular velocity reaches the final value at steady state for the robust controller (CSMC) but at the time = 200 s, at steady state, this design chose adjusting the set point with $x_{2d} = -20.944\ \text{rad/s}$. As a result, the angular velocity reaches another final value at steady state for the robust controller (CSMC) with high stability and performance as shown in Fig. 9. This demonstrates that the proposed controller can meet various operational requirements. The response results of the robust controller are shown in Table IX.

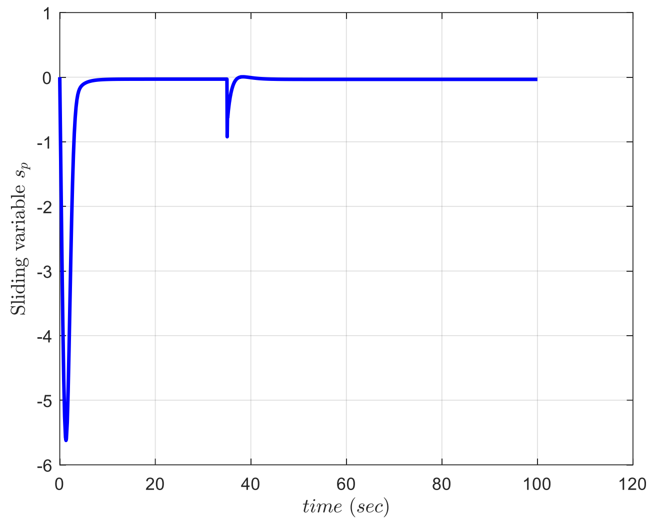

Fig. 8. The sliding variable s_p time response of closed-loop with robust controller with torque disturbances effects

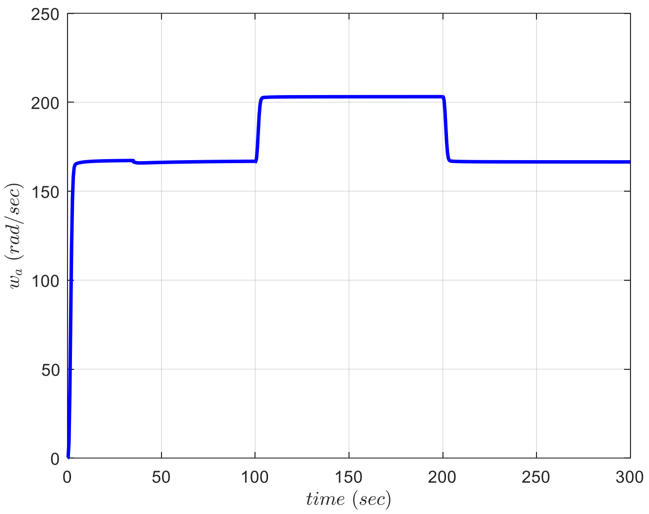

Fig. 9. The velocity time response of multi steps for closed-loop with robust controllers with torque disturbances

TABLE IX. RESULTS OF VELOCITY TIME RESPONSE OF MULTI STEPS FOR ROBUST CONTROLLER

Robust Controller	Steady state value with set point (167.5516 rad/sec)	Steady state value with increasing set point (36.6519 rad/sec)	Error steady state with increasing set point (36.6519 rad/sec)	Steady state value with decreasing set point (−20.944 rad/sec)	Error steady state with decreasing set point (−20.944 rad/sec)
CSMC	166.8 rad/sec	203.4 rad/sec	0.0519 rad/sec	182.456 rad/s	0.544 rad/sec

At the time = 100 s, at steady state, this design chose increasing the set point with $x_{2d} = 36.6519\ \mathrm{rad/s}$. As a result, the pressure supply reaches a final value at steady state for the robust controller (CSMC) but at the time = 200 s, at steady state, this design chose adjusting the set point with $\mathrm{x}_{2\mathrm{d}} = -20.944\ \mathrm{rad/s}$. As a result, the pressure supply reaches another final value at steady state for the robust controller (CSMC) with high stability and performance as shown in Fig. 10. This demonstrates that the proposed controller can meet various operational requirements. The response results of the robust controller are shown in Table X.

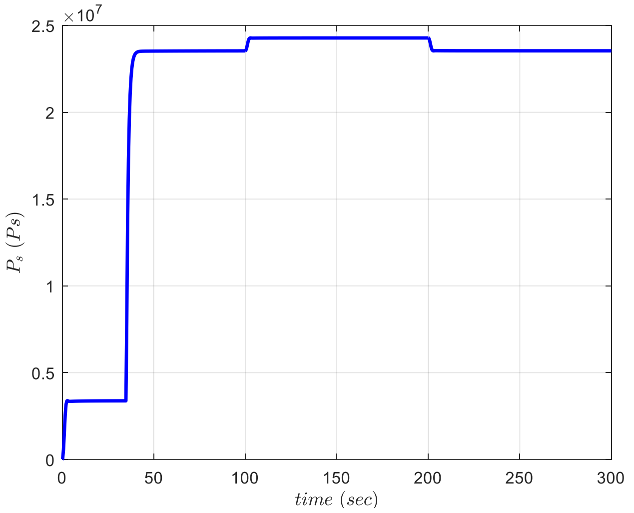

Fig. 10. The pressure supply time response of multi steps for closed-loop with robust controller with torque disturbances

TABLE X. RESULTS PRESSURE SUPPLY TIME RESPONSE OF MULTI STEPS FOR ROBUST CONTROLLER

Robust Controller	Steady state value with set point (167.5516 rad/sec)	Steady state value with increasing set point (36.6519 rad/sec)	Steady state value with decreasing set point (−20.944 rad/sec)
CSMC	23.54 MP	24.28 MP	23.86 MP

At the time = 100 s, at steady state, this design chose increasing the set point with $\mathrm{x}_{2\mathrm{d}} = 36.6519\ \mathrm{rad/s}$. As a result, the valve opening area reaches a final value at steady state for all the robust controllers (CSMC) but at the time = 200 s, at steady state, this design chose adjusting the set point with $\mathrm{x}_{2\mathrm{d}} = -20.944\ \mathrm{rad/s}$. As a result, the valve opening area reaches another final value at steady state for the robust controller (CSMC) with high stability and performance as shown in Fig. 11. This demonstrates that the proposed controllers can meet various operational requirements. The response results of the robust controller are shown in Table XI.

TABLE XI. RESULTS OF OPENING AREA TIME RESPONSE OF MULTI STEPS FOR ROBUST CONTROLLER

Robust Controller	Steady state value with set point (167.5516 rad/sec)	Steady state value with increasing set point (36.6519 rad/sec)	Steady state value with decreasing set point (−20.944 rad/sec)
CSMC	$5.892 \times 10^{-6}\mathrm{m}^2$	$7.042 \times 10^{-6}\mathrm{m}^2$	$6.382 \times 10^{-6}\mathrm{m}^2$

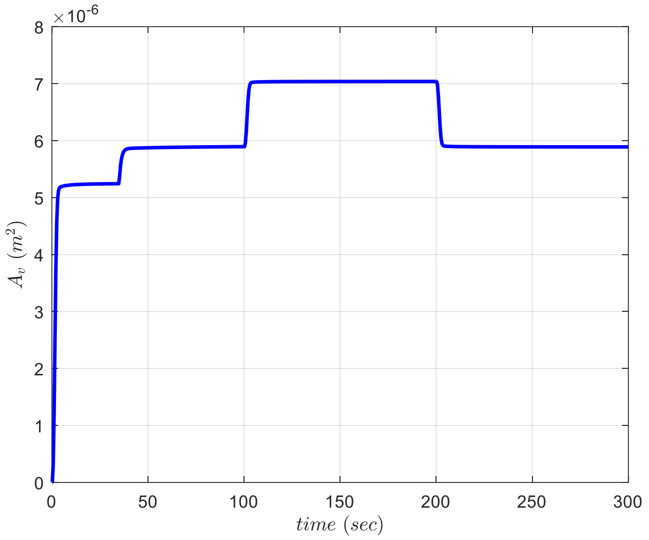

Fig. 11. The valve opening area time response of multi steps for robust controllers with torque disturbances effects

At the time = 100 s, at steady state, this design chose increasing the set point with $\mathrm{x}_{2\mathrm{d}} = 36.6519\ \mathrm{rad/s}$. As a result, the control action reaches a final value at steady state for all the robust controllers (CSMC) but at the time = 200 s, at steady state, this design chose adjusting the set point with $\mathrm{x}_{2\mathrm{d}} = -20.944\ \mathrm{rad/s}$. As a result, the valve opening area reaches another final value at steady state for the robust controller (CSMC) with high stability and performance as shown in Fig. 12. This demonstrates that the proposed controller can meet various operational requirements. The response results of the robust controller are shown in Table XII.

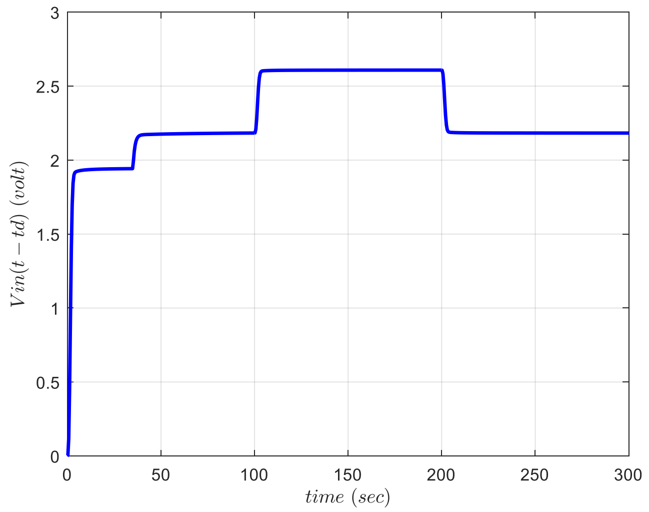

Fig. 12. The control action time response of multi steps for robust controllers with torque disturbances effects

TABLE XII. RESULTS OF MULTI STEPS CONTROL ACTION TIME RESPONSE OF MULTI STEPS WITH ROBUST CONTROLLER

Robust Controller	Steady state value with set point (167.5516 rad/sec)	Steady state value with increasing set point (36.6519 rad/sec)	Steady state value with decreasing set point (−20.944 rad/sec)
CSMC	2.182 volt	2.608 volt	2.365 volt

Case3: Control robustness under parameters uncertainty. For CSMC, Fig. 13 to Fig. 16, show the time response of the uncertain system with multiplicative uncertainty. The uncertainties were determined based on errors in uncertain parameters of nominal system within the range of ±10% of the nominal values for the six parameters of the system. It could be noticed that the system has good performance within the whole uncertainty set. Note the responses stayed have high stability and performance although the high uncertainties. Note that the effects of the multiplicative uncertainty on the system for controller CSMC less than the effects it on the system for linear robust controllers.

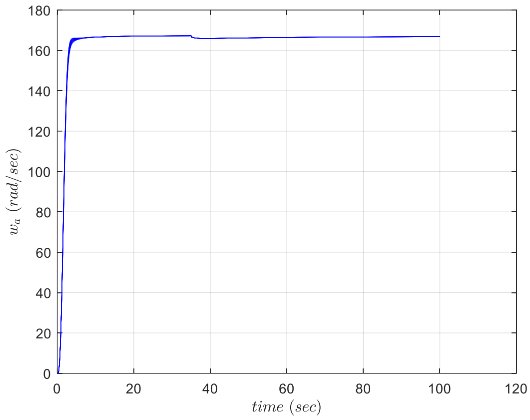

Fig. 13. The perturbed velocity time response for closed-loop with (CSMC) and disturbances effects

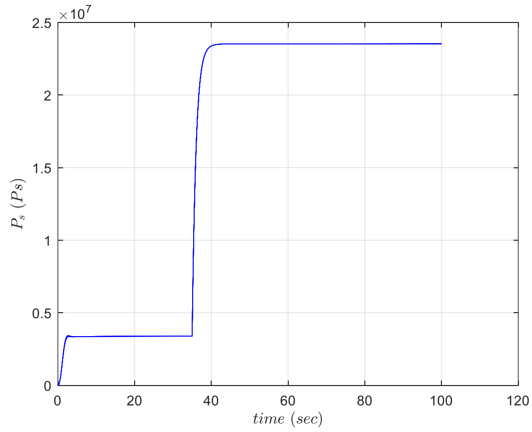

Fig. 14. The perturbed pressure supply time response for closed-loop with (CSMC) and disturbances effects

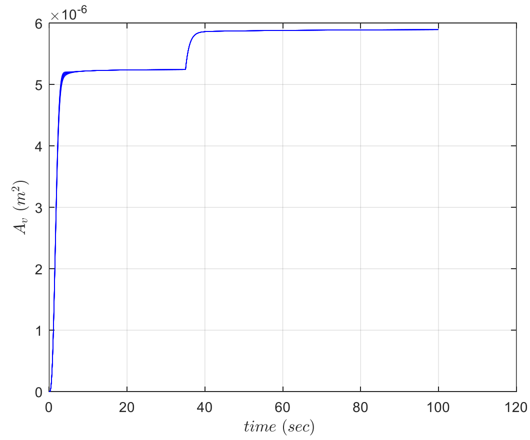

Fig. 15. The perturbed valve opening area time response for closed-loop with (CSMC) and disturbances effects

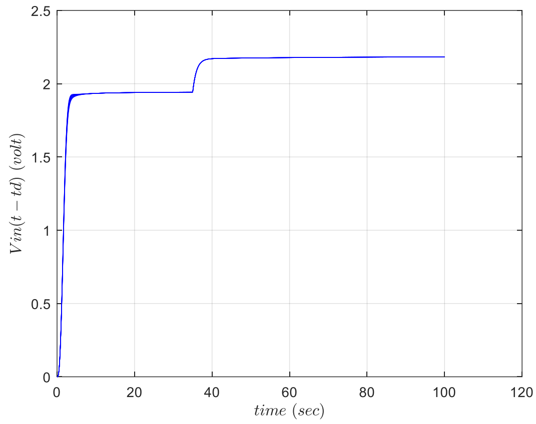

Fig. 16. The perturbed control action time response for closed-loop with (CSMC) and disturbances effects

VIII. CONCLUSIONS

This work presents a design of the Backstepping sliding mode Controller for controlling the angular velocity control for a rotary actuator. The controlled system's stability analysis has been presented using the Lyapunov Function. Two switching functions for two level subsystems; low level subsystem and high level subsystem have been constructed where the back-stepping was used in the conventional sliding mode control. The simulation results demonstrated that the Backstepping Sliding Mode Controller ensures robust stability and meets the desired time-domain specifications with uncertainties and disturbances. The simulation results have been obtained based on the MATLAB software tools, showed no settling time, eliminating steady state error, no overshoot, as well as high responsiveness in tracking the reference speed in spite of the variation in parameters and external torque disturbance. The simulation results show the Backstepping sliding mode controller has a better robustness in terms of stability and performance in comparison with the robust controllers based on linear control techniques. The simulation results demonstrated that the Backstepping Sliding Mode controller ensure robust stability and performance of the system in the time-domain specifications with multiplicative uncertainties and disturbances. The proposed controller can meet various operational requirements. The system with Backstepping sliding mode controller has fast response to track the reference step value in spite of the variation in parameters and external torque disturbance.

The effects of the multiplicative uncertainty on the system with controllers CSMC little. The Backstepping conventional sliding mode controller has a high robustness in terms of stability and performance in comparison with the robust controllers based on linear control techniques. Future work emphasize on merging the robust controllers based on linear control techniques with Backstepping sliding mode controller in the inlet throttling velocity control system for increasing robustness for the stability and performance in addition to effectiveness.

Future work emphasize on employing fuzzy logic, neural network and adaptive control in the inlet throttling velocity control system. The fuzzy logic is used for a wide range of applications, including control systems, decision-making, pattern recognition, and artificial intelligence. The neural networks are used for solving complex problems and driving innovation in many areas. The adaptive control is used as a powerful and flexible approach to control system design, providing improved performance, robustness, and adaptability in a wide range of applications.

REFERENCES

[1] Z. Jing and H. Qi, “Design and Calculation of Hydraulic Transmission System of Loader," *MMEAT 2020 Journal of Physics: Conference Series*, vol. 1676, p. 012242, 2020.

[2] H. H. Ali and R. C. Fales, “A review of flow control methods,” *International Journal of Dynamics and Control*, vol. 9, pp. 1847–1854, 2021.

[3] P. O. Kaltjob. *Control of Mechatronic Systems: Model-Driven Design and Implementation Guidelines*. John Wiley & Sons, 2020.

[4] X. Ji, C. Wang, Z. Zhang, S. Chen, and X. Guo, “Nonlinear adaptive position control of hydraulic servo system based on sliding mode back-stepping design method,” *Proceedings of the Institution of Mechanical Engineers, Part I: Journal of Systems and Control Engineering*, vol. 235, no. 4, pp. 474-485, 2021.

[5] S. Koch and M. Reichhartinger, “Observer-based sliding mode control of hydraulic cylinders in the presence of unknown load forces,” *Elektrotech. Informationstechnik*, vol. 133, no. 6, pp. 253-260, 2016.

[6] S. A. AL-Samarraie, S. M. Mahdi, T. M. M. Ridha, and M. H. Mishary, “Sliding mode control for electro-hydraulic servo system,” *Iraqi J Comput Commun Control Syst Eng*, vol. 15, no. 3, pp. 1-10, 2015.

[7] Z. Zheng, “Disturbance-Observer-Based Global Sliding Mode Controller for Electro-Hydraulic System,” *International Journal of Control and Automation*, vol. 9, no. 12, pp. 117-124, 2016.

[8] A. M. Mohammad and S. A. AL-Samarraie, “Robust controller design for flexible joint based on back-stepping approach,” *Iraqi Journal of Computers, Communications, Control and Systems Engineering*, vol. 20, no. 2, pp. 58-73, 2020.

[9] A. Esatoglu and M. U. Salamci, “Sliding Mode Control Design for a Two-Stage of Electro-Hydraulic Valve,” in *Proceedings of the 3rd International Conference on Vision, Image and Signal Processing*, pp. 1-6, 2019.

[10] A. K. Hamoudi and L. T. Rasheed, “Design and implementation of adaptive backstepping control for position control of propeller-driven pendulum system,” *Journal Européen des Systèmes Automatisés*, vol. 56, no. 2, p. 281, 2023.

[11] W. Xingxu, H. Guang, and G. Rui, “PID Sliding Mode Control for Electro-hydraulic Servo System,” *IOP Conf.Series: Journal of Physics: Conf. Series*, vol. 1168, p. 022085, 2019.

[12] Y. Jing, Y. -e. Mao, G. M. Dimirovski, Y. Zheng, and S. Zhang, "Adaptive global sliding mode control strategy for the vehicle antilock braking systems," *2009 American Control Conference*, pp. 769-773, 2009, doi: 10.1109/ACC.2009.5160357.

[13] Y. Mingxing, Q. Zhang, L. U. Xinliang, X. I. Ruru, and W. Xingsong, “Adaptive sliding mode control of a nonlinear electro-hydraulic servo system for position tracking,” *Mechanics*, vol. 25, no. 4, pp. 283-290, 2019.

[14] A. Esatoglu and M. U. Salamci, “Sliding Mode Control Design for a Two-Stage of Electro-Hydraulic Valve,” in *Proceedings of the 3rd International Conference on Vision, Image and Signal Processing*, pp. 1-6, 2019.

[15] S. Parvaze *et al*., "Optimization of Water Distribution Systems Using Genetic Algorithms: A Review," *Archives of Computational Methods in Engineering*, vol. 30, no. 7, pp. 4209-4244, 2023.

[16] E. Dejband, Y. C. Manie, Y. J. Deng, M. A. Bitew, T. H. Tan, and P. C. Peng, "High Accuracy and Cost-Effective Fiber Optic Liquid Level Sensing System Based on Deep Neural Network," *Sensors*, vol. 23, no. 4, 2023.

[17] C. Urrea and Y. Garcia-Garcia, "Design and Performance Analysis of Level Control Strategies in a Nonlinear Spherical Tank," *Processes*, vol. 11, no. 3, 2023.

[18] Q. Wang, H. Chen, and W. Zhang, "Robust Sliding Mode Control for Nonlinear Two-Tank Liquid Level Systems," *IEEE Access*, vol. 10, pp. 151730-151743, 2022, doi: 10.1109/ACCESS.2022.3202317.

[19] E. Mehri and M. Tabatabaei, "Control of quadruple tank process using an adaptive fractional-order sliding mode controller," *Journal of Control, Automation and Electrical Systems*, vol. 32, pp. 605-614, Jun. 2021.

[20] T. Dlabač, S. Antić, M. Ćalasan, A. Milovanović, and N. Marvučić, "Nonlinear tank-level control using Dahlin algorithm design and PID control," *Applied Sciences*, vol. 13, no. 9, p. 5414, Apr. 2023, doi: 10.3390/app13095414.

[21] S. B. Joseph, E. G. Dada, A. Abidemi, D. O. Oyewola, and B. M. Khammas, “Metaheuristic algorithms for PID controller Parameters tuning: Review, approaches and open problems,” *Heliyon*, vol. 8, no. 5, May 2022, doi: 10.1016/j.heliyon. 2022.e09468.

[22] Z. O. Barambones, J. A. Cortajarena, and P. Alkorta, "New control schemes for actuators," in *Actuators*, vol. 13, no. 3, p. 99, Mar. 2024.

[23] F. Xu, Z. Sui, Y. Wang, and J. Xu, "An improved data-driven integral sliding-mode control and its automation application,"*Applied Sciences*, vol. 13, no. 24, p. 13094, Dec. 2023, doi: 10.3390/app132413094.

[24] P. Jiang, "Summary of PID control system of liquid level of a single-capacity tank," *Journal of Physics: Conference Series*, vol. 1865, no. 2, p. 022061, 2021.

[25] T. K. Sundari, R. Giri, M. G. Umamaheswari, S. Durgadevi, and C. Komathi, "Fuzzy Logic Control of Liquid Level in a Single Tank with IoT-Based Monitoring System," in *ICDSMLA 2021: Proceedings of the 3rd International Conference on Data Science, Machine Learning and Applications*, pp. 401-414, 2023.

[26] W. Wang, X. Zhang, L. Li, and Z. Liu, "Unrefined slippery mode control of nonlinear two-tank liquid-level systems," *International Journal of Science and Research*, vol. 4, no. 8, pp. 618-623, 2015.

[27] Y. Zhang and J. Liu, "Fractional-Order Sliding Mode Control of Two-Tank Liquid Level Systems," *Nonlinear Dynamics*, vol. 102, no. 1-2, pp. 1219-1234, 2022.

[28] S. Li and Y. Wu, "Adaptive Sliding Mode Control of Two-Tank Liquid Level Systems with Uncertainties," *Journal of Process Control*, vol. 111, pp. 1-10, 2023, doi: 10.1016/j.jprocont.2023.05.002.

[29] Z. Wang and H. Zhang, "Event-Triggered Sliding Mode Control for Two-Tank Liquid Level Systems with Networked Communication," *ISA Transactions*, vol. 125, pp. 339-350, 2023, doi: 10.1016/j.isatra.2022.12.030.

[30] Y. Xu and M. Sun, "Integral Sliding Mode Control for Two-Tank Liquid Level Systems with Input Constraints," *Control Engineering Practice*, vol. 118, 2024, doi: 10.1016/j.conengprac.2022.104817.

[31] S. Mondal and S. Sarkar, "Hybrid Fuzzy Sliding Mode Controller for a Coupled Tank System," *Journal of Control, Automation and Electrical Systems*, vol. 30, no. 3, pp. 299-312, Jun. 2019.

[32] Z. S. Hashim, H. I. Khani, A. T. Azar, Z. I. Khan, D. A. Smait, and A. Abdulwahab, "Robust liquid level control ofquadruple tank system: A nonlinear model-free approach," *Actuators*, vol. 12, no. 3, 2023, doi: 10.3390/act12030119.

[33] H. H. Ali, R. C. Fales, and N. D. Manring, "Modeling and control design for an inlet metering valve-controlled pump that controls actuator velocity via H-infinity and two-degrees-of-freedom methods," *Heliyon*, vol. 10, no. 2, p. e26223, 2019.

[34] T. Nguyen and K. Uchida, "Optimal Control for Fluid Level Systems Using Model Predictive Control," *Journal of Process Control*, vol. 72, pp. 32-40, Oct. 2019, doi: 10.1016/j.jprocont.2018.12.003.

[35] H. J. Marquez. *Nonlinear Control Systems: Analysis and Design*. Hoboken, NJ: Wiley, 2020.

[36] Y. Wang, "Reinforcement Learning for Adaptive Control of Fluid Level Systems," *IEEE Transactions on Systems, Man, and Cybernetics: Systems*, vol. 50, no. 5, pp. 2783-2792, May 2020, doi: 10.1109/TSMC.2020.2973927.

[37] A. H. Hamzah and S. Z. H. Noor, "Intelligent Control of Fluid Level Systems with IoT Integration," *IEEE Internet of Things Journal*, vol. 8, no. 10, pp. 8271-8282, Oct. 2021, doi: 10.1109/JIOT.2021.3057243.

[38] G. H. Pham, "Hybrid Fuzzy-PID Control for Fluid Level Systems," *International Journal of Fuzzy Systems*, vol. 22, no. 4, pp. 1234-1244, Apr. 2020.

[39] M. S. Ali, "Sliding Mode Control for Mechatronic Systems: A Review," *IEEE Access*, vol. 8, pp. 169691-169709, Sep. 2020, doi: 10.1109/ACCESS.2020.3012343.

[40] H. H. Ali, F. M. Abdulsattar, and A. W. Mustafa, "A New Mechanical Analysis of a Crankshaft-connecting Rod Dynamics Using Lagrange's Trigonometric Identities," *Journal of Engineering & Technological Sciences*, vol. 54, no. 2, 2022.

[41] R. T. Saravanan, "Adaptive Sliding Mode Control for Nonlinear Fluid Level Systems," *ISA Transactions*, vol. 95, pp. 45-55, Sep. 2019, doi: 10.1016/j.isatra.2019.03.002.

[42] Z. Wu and L. Zhang, "Model Predictive Control for Nonlinear Fluid Level Systems with Disturbance Rejection," *IEEE Transactions on Control Systems Technology*, vol. 30, no. 5, pp. 1711-1722, Sep. 2022, doi: 10.1109/TCST.2021.3089318.

[43] J. Y. Hung and W. Gao, "Variable Structure Control: A Survey," *IEEE Transactions on Industrial Electronics*, vol. 40, no.1, pp. 2-22, Feb. 2020, doi: 10.1109/41.184818.

[44] A. J. Humaidi, M. Riyadh Hameed, A. R. Ajel, A. Hashim Hameed, A. A. Al-Qassar, and I. Kasim Ibraheem, "Block Backstepping Control Design of Two-Wheeled Inverted Pendulum Via Zero Dynamic Analysis," *2021 IEEE 12th Control and System Graduate Research Colloquium (ICSGRC)*, pp. 87-92, 2021, doi: 10.1109/ICSGRC53186.2021.9515308.

[45] A. K. Mishra, "Fuzzy Logic Control System and its Applications," *Int. Res. J. Eng. Technol.*, vol. 2, no. 8, pp. 742-746,2015.

[46] K. S. Narendra and A. M. Annaswamy. *Stable Adaptive Systems*. Englewood Cliffs, NJ: Prentice Hall, 2019.

[47] L. A. Zadeh, "Fuzzy Sets," *Information and Control*, vol. 8, no. 3, pp. 338-353, June 1965.

[48] J. C. Doyle, B. A. Francis, and A. R. Tannenbaum. *Feedback Control Theory*. New York: Macmillan, 2021.

[49] S. S. Sastry. *Adaptive Control: Stability, Convergence, and Robustness*. Englewood Cliffs, NJ: Prentice-Hall, 2022.

[50] Y. Su, "Artificial Intelligence Techniques in Control Systems: A Review," *IEEE Transactions on Systems, Man, and Cybernetics*, vol. 51, no. 6, pp. 3911-3927, Dec. 2021, doi: 10.1109/TSMC.2021.3072157.

[51] R. Isermann. *Adaptive Control and Fault Diagnosis*. Trends in Advanced Control and Applications pp. 83-114, Berlin: Springer, 2019.

[52] J. J. E. Slotine and W. Li. *Applied Nonlinear Control*. Englewood Cliffs, NJ: Prentice-Hall, 2021.

[53] W. R. Abdul-Adheem *et al*., "Anti-disturbance compensation-based nonlinear control for a class of MIMO uncertain nonlinear systems" *Entropy*, vol. 23, no. 11, p. 1487, 2021.

[54] M. J. Yazdanpanah and M. Tatari, "Robust Control of Nonlinear Systems: Applications to Fluid Level Systems," *Automatica*, vol. 80, pp. 115-123, Jun. 2019, doi: 10.1016/j.automatica.2017.02.012.

[55] S. Dodds. *The Generalized PI Controller*. Feedback Control: Linear, Nonlinear, and Robust Techniques and Design with Industrial Applications pp. 55-102, New York: Springer, 2022.

[56] C. A. Guldemir, "Sliding Mode Control in Robotics: Application to Fluid Level Systems," in *Proceedings of the 2018 IEEE/RSJ International Conference on Intelligent Robots and Systems (IROS)*, pp. 2314-2319, 2019, doi:10.1109/IROS.2018.8543773.

[57] B. R. Barmish. *Adaptive Control of Uncertain Systems*. Englewood Cliffs, NJ: Prentice Hall, 2021.

[58] H. K. Khalil. *Nonlinear Systems Third Edition*. Prentice Hall Prentice-Hall, Inc. Upper Saddle River, 1996.

[59] C. A. Guldemir, "Sliding Mode Control in Robotics: Application to Fluid Level Systems," in *Proceedings of the 2018 IEEE/RSJ International Conference on Intelligent Robots and Systems (IROS)*, pp. 2314-2319, 2019, doi:10.1109/IROS.2018.8543773.

[60] B. R. Barmish. *Adaptive Control of Uncertain Systems*. Englewood Cliffs, NJ: Prentice Hall, 2021.

[61] A. Khadraoui, M. Zribi, and M. Mnif, "Sliding mode control of a class of nonlinear systems with application to a fluid level process," *International Journal of Control*, vol. 75, no. 9, pp. 622-634, Jun. 2020, doi: 10.1080/00207170210133047.

[62] A. Isidori. *Nonlinear Control Systems, 3rd ed*. Berlin: Springer, 2021.

[63] K. Ogata. *Modern Control Engineering, 5th ed*. Upper Saddle River, NJ: Prentice Hall, 2020.

[64] J. Feng, W. Wang, and H. -B. Zeng, "Integral Sliding Mode Control for a Class of Nonlinear Multi-Agent Systems With Multiple Time-Varying Delays," in *IEEE Access*, vol. 12, pp. 10512-10520, 2024, doi: 10.1109/ACCESS.2024.3354030.

[65] W. Tan, "Tuning of PID controllers for open-loop unstable processes: A summary," *Control Engineering Practice*, vol. 16, no. 9, pp. 1069-1076, Sep. 2020, doi: 10.1016/j.conengprac.2007.12.008.

[66] C. S. Rao and S. Santosh, "Tuning optimal PID controllers for open loop unstable first order plus time delay systems by minimizing ITAE criterion," *IFAC-PapersOnLine*, vol. 53, no. 1, pp. 123-128, 2020.

[67] L. T. Rasheed and M. K. Hamzah, "Design of an optimal backstepping controller for nonlinear system under disturbance," *Engineering and Technology Journal*, vol. 39, no. 3, pp. 465-476, 2021.

[68] A. Humaidi and M. Hameed, "Development of a new adaptive backstepping control design for a nonstrict and under-actuated system based on a PSO tuner," *Information*, vol. 10, no. 2, p. 38, 2019.

[69] S. S. Mukhopadhyay, "A comparison of intelligent controllers in control of a nonlinear inverted pendulum system,"*Measurement*, vol. 46, no. 10, pp. 4211-4224, Dec. 2019, doi: 10.1016/j.measurement.2013.07.041.

[70] A. K. Sharma, "PID Control for Linear Systems: An Overview," *Control Engineering Journal*, vol. 55, no. 1, pp. 12-21, 2019, doi: 10.1016/j.cej.2019.05.012.

[71] M. D. Chen, "Sliding Mode Control in Uncertain Systems," *International Journal of Control*, vol. 98, no. 2, pp. 33-44, 2020.

[72] B. X. Liu, "Hybrid PID-SMC Controller for Liquid Level Processes," *Industrial Process Control*, vol. 67, no. 3, pp. 88-95, 2020, doi: 10.1109/TIE.2020.2345678.

[73] P. L. Gomez, "Performance Enhancement of Hybrid PID-SMC Systems," *IEEE Trans. Ind. Electron*., vol. 67, no. 5, pp. 454-463, 2021, doi: 10.1109/TIE.2021.1234567.

[74] C. G. Lee, "Adaptive Control in Nonlinear Liquid Level Systems," *Automation and Control Engineering Journal*, vol. 69, no. 2, pp. 201-210, 2021.

[75] S. R. Patel, "Chattering Mitigation in Sliding Mode Control for Industrial Processes," *Journal of Dynamic Systems*, vol. 45, no. 2, pp. 145-153, 2022.

[76] J. N. White, "Adaptive PID Controllers in Time-Varying Systems," *Journal of Process Automation*, vol. 56, no. 4, pp. 321-330, 2020, doi: 10.1016/j.jprocont.2020.05.001

[77] Z. A. Waheed *et al.*, "Control Of Elbow Rehabilitation System Based On Optimal-Tuned Backstepping Sliding Mode Controller," *Journal of Engineering Science and Technology*, vol. 18, no. 1, pp. 584–603, 2023.

[78] E. K. Gupta, "Robust Control for Enhanced Disturbance Rejection in PID Systems," *Journal of Control Systems*, vol. 74, no. 1, pp. 11-23, 2022, doi: 10.1109/JCS.2022.1021032

[79] H. Y. Zhao, "Advances in Sensor Technologies for Hybrid Controllers," *Sensors and Control Systems*, vol. 68, no. 3, pp. 421-432, 2021.

[80] C. C. Lee, "Fuzzy Logic in Control Systems: Fuzzy Logic Controller—Part I," *IEEE Transactions on Systems, Man, and Cybernetics*, vol. 20, no. 2, pp. 404-418, Mar. 2020.

[81] S. V. Emelyanov, "High-order sliding modes in Control systems," *Computational Mathematics and Modeling*, vol. 18, no. 1, pp. 6-15, Jan. 2020.

[82] J. W. Bennett, "Sliding Mode Control for Fluid Level Systems: A Robust Approach," *IEEE Transactions On Control Systems Technology*, vol. 23, no. 3, pp. 1114-1122, May 2020, doi: 10.1109/TCST.2014.2362511.

[83] M. H. Lee and H. S. Kim, "Design of Adaptive Sliding Mode Controller for Fluid Level Systems," *Control Engineering Practice*, vol. 22, no. 12, pp. 1577-1585, Dec. 2020, doi: 10.1016/j.conengprac.2014.09.007.

[84] T. D. Nguyen, "Adaptive Neural-Fuzzy Control of Fluid Level Systems," *Neural Computing and Applications*, vol. 32, no. 1, pp. 231-244, Jan. 2020, doi: 10.1007/s00521-019-04122-1.

[85] R. K. Singh, "IoT-Based Real-Time Monitoring Systems in Liquid Level Control," *International Journal of Control Systems*, vol. 73, no. 6, pp. 289-300, 2020, doi: 10.1080/00207179.2020.1847619

[86] D. C. Moon, "Adaptive Control Actions in Hybrid PID-SMC Controllers," *Journal of Engineering Systems*, vol. 67, no. 7, pp. 205-214, 2021, doi: 10.1109/TIE.2021.3071149

[87] S. A. Al-Samarraie, “Invariant sets in sliding mode control theory with application to servo actuator system with friction,” *WSEAS Transactions on Systems and Control*, vol. 8, no. 2, pp. 33-45, 2013.

[88] S. M. Al-Karawi, "Simulation Study of Hybrid Control in Liquid Level Systems," *Automation and Control Technology*, vol. 64, no. 2, pp. 125-134, 2020, doi: 10.1109/TAC.2020.1234567

[89] K. W. Li, "Adaptability of Hybrid Controllers in Industrial Applications," *IEEE Trans. Ind. Syst.*, vol. 74, no. 3, pp. 245-256, 2022, doi: 10.1109/TIS.2022.1234567

[90] F. H. Chung, "Machine Learning Techniques for Controller Optimization," *Journal of Process Control Engineering*, vol. 71, no. 4, pp. 312-322, 2023, doi: 10.1016/j.jprocont.2023.05.002-z.